Unified Analysis of Switched Diversity Systems in Independent and Correlated Fading Channels

Chinthananda Tellambura, *Member, IEEE*, A. Annamalai, *Member, IEEE*, and Vijay K. Bhargava, *Fellow IEEE*

***Abstract*—The moment generating function (MGF) of the signal power at the output of dual-branch switch-and-stay selection diversity (SSD) combiners is derived. The first-order derivative of the MGF with respect to the switching threshold is also derived. These expressions are obtained for the general case of correlated fading and nonidentical diversity branches, and hold for any common fading distributions (e.g., Rayleigh, Nakagami-m, Rician, Nakagami-q). The MGF yields the performance (bit or symbol error probability) of a broad class of coherent, differentially coherent and noncoherent digital modulation formats with SSD reception. The optimum switching threshold (in a minimum error rate sense) is obtained by solving a nonlinear equation which is formed by using the first-order derivative of the MGF. This nonlinear equation can be simplified for several special cases. For independent and identically distributed diversity branches, the optimal switching threshold in closed form is derived for three generic forms of the conditional error probability. For correlated Rayleigh or Nakagami-m fading with identical branches, the optimal switching threshold in closed form is derived for the noncoherent binary modulation formats. We show previously published results as special cases of our unified expression. Selected numerical examples are presented and discussed.**

***Index Terms*—Diversity reception, mobile radio systems, switched diversity.**

I. Introduction

TESTIMONIES OF "wireless catching up with wireline" have begun. However, the nonstationary and hostile nature of wireless channels impose the greatest threat to reliable data transmission over wireless links. The performance of a digital modulation scheme is degraded by many transmission impairments including fading, delay spread, cochannel interference and noise. Diversity reception is a classical yet powerful communication receiver technique that provides wireless link improvement at relatively low cost. Among the various known diversity combining methods, selection diversity is the simplest and perhaps the most frequently used in practice. For instance, a form of selection diversity has been implemented in one current digital cellular system (specified in the IS-54 common air interface) where the diversity branch is selected prior to thetransmission of a TDMA burst. Furthermore, the ideal selective combining (SDC) that selects the branch with the highest signal-to-noise ratio (SNR) may not be practical for radio links that use continuous transmission (e.g., FDMA systems) because it requires continuous monitoring of all the diversity branches. This problem can be circumvented by adopting a suboptimal switched diversity scheme.

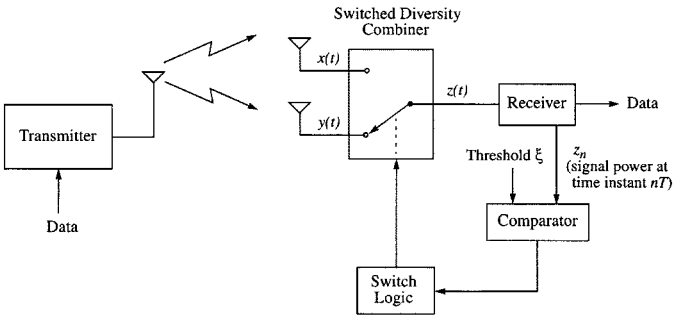

Fig. 1. Block diagram of a predetection switched diversity system.

Consider a two-branch switched diversity system depicted in Fig. 1. If the instantaneous envelope of the received signal falls below a predetermined threshold, the antenna switch is triggered, thus selecting the second branch. If the second branch is above the threshold, switching ceases. If the second branch is also in a fade, we can immediately revert to the first branch, and if necessary, continue the rapid switching between the two antennas until one of them emerges above the threshold (i.e., switch-and-examine strategy), or we may switch to the second branch and remain there at least until the next switching instant regardless whether the instantaneous signal power in the second antenna is above or below the threshold (i.e., switch-and-stay strategy). Moreover, the switched diversity system has the advantage that only a single intermediate-frequency circuitry and a receiver "front-end" are used, thus avoiding the expense of extra diplexers and other high-frequency analog circuits.

Previous related studies on switched diversity systems include the following: In [1], Rustako *et al.* theoretically and experimentally examined a switched diversity system on independent Rayleigh channels using a continuous time signal model. In their switch-and-stay strategy, switching between the two antennas only occurs if there is a downward threshold crossing. Shortall [2] builds a prototype of a switched diversity system and experimentally examines the effect of the signal correlation on the receiver performance. Subsequently, Adachi *et al.* [3] investigated the performance of a periodic switching diversity technique using digital FM with discriminator detection on Rayleigh fading channels. Blanco and Zdunek [4] theoretically

Paper approved by N. C. Beaulieu, the Editor for Wireless Communication Theory of the IEEE Communications Society. Manuscript received January 31, 1999; revised March 29, 2001.

C. Tellambura is with the Faculty of Information Technology, Monash University, Clayton, Vic. 3168, Australia (e-mail: chintha@csse.monash.edu.au).

A. Annamalai is with The Bradley Department of Electrical and Computer Engineering, Virginia Polytechnic Institute and State University, Alexandria, VA 22314 USA (e-mail: annamalai@vt.edu).

V. K. Bhargava is with the Department of Electrical and Computer Engineering, University of Victoria, Victoria, BC V8W 3P6, Canada (e-mail: bhargava@engr.uvic.ca).

Publisher Item Identifier S 0090-6778(01)10176-5.

TABLE I
INSTANTANEOUS SER OF SEVERAL COMMON MODULATION SCHEMES

Modulation Scheme	Conditional Error Probability $P_S(\varepsilon\mid\gamma)$
Coherent binary signalling:	
(a) Coherent PSK	$0.5\mathrm{erfc}(\sqrt{\gamma})$
(b) Coherent detection of differentially encoded PSK	$\mathrm{erfc}(\sqrt{\gamma})-\frac{1}{2}\mathrm{erfc}^2(\sqrt{\gamma})$
(c) Coherent FSK	$0.5\mathrm{erfc}(\sqrt{\gamma/2})$
Noncoherent binary signalling:	
(a) DPSK	$0.5\exp(-\gamma)$
(b) Noncoherent FSK	$0.5\exp(-\gamma/2)$
Quadrature signalling:	
(a) QPSK	$\mathrm{erfc}(\sqrt{\gamma})-0.25\mathrm{erfc}^2(\sqrt{\gamma})$
(b) MSK	$\mathrm{erfc}(\sqrt{\gamma})-0.25\mathrm{erfc}^2(\sqrt{\gamma})$
(c) $\pi/4$-DQPSK with Gray coding [10]	$\frac{1}{2\pi}\int_0^{\pi}\frac{\exp(-\gamma(2-\sqrt{2}\cos\theta))}{\sqrt{2}-\cos\theta}d\theta$
Multilevel signalling:	
(a) Square QAM	$2q\mathrm{erfc}(\sqrt{p\gamma})-q^2\mathrm{erfc}^2(\sqrt{p\gamma})$ where $q=1-1/\sqrt{M}$ and $p=1.5\log_2 M/(M-1)$
(b) MPSK	$\frac{1}{\pi}\int_0^{\pi-\pi/M}\exp\left(\frac{-\gamma\sin^2(\pi/M)\log_2 M}{\sin^2\theta}\right)d\theta$
(c) MDPSK [12]	$\frac{\sin(\pi/M)}{\pi}\int_0^{\pi/2}\frac{\exp(-\gamma\log_2 M[1-\cos(\pi/M)\cos\theta])}{1-\cos(\pi/M)\cos\theta}d\theta$ or $\frac{1}{\pi}\int_0^{\pi-\pi/M}\exp\left(\frac{-\gamma\sin^2(\pi/M)\log_2 M}{1+\cos(\pi/M)\cos\theta}\right)d\theta$
(d) Two-dimension M-ary signal constellations [13]	$\frac{1}{2\pi}\sum_{k=1}^{N}Pr(S_k)\int_0^{\eta_k}\exp\left(\frac{-\gamma\alpha\sin^2(\Psi_k)}{\sin^2(\theta+\Psi_k)}\right)d\theta$ where N is the number of signal points, and $Pr(S_k)$ is the *a priori* probability that the kth signal point is transmitted.

examined the performance of a switched diversity system initially proposed in [1] for noncoherent frequency-shift keying (NCFSK) in independent Rayleigh fading channels based on a discrete-time approach. Their analysis was extended in [5] for the Nakagami-m fading channels.

In [6], Abu-Dayya and Beaulieu proposed a different switch-and-stay strategy (which is referred to as SWC in this paper) and analyzed the performance of binary NCFSK on Nakagami-m fading channels based on a discrete-time model. Different from [4], the antenna switch in the SWC scheme is activated in the next switching instant as long as the measured local power in the current antenna is below the threshold level (i.e., the envelope of the received signal need not necessarily cross the threshold in the negative direction). Therefore, it does not require comparison of present samples with past samples. Moreover, the rate of branch switching is reduced with respect to the ideal selection diversity, which translates into a reduction of transient effects due to switching. Their analysis for both independent and correlated Nakagami-m signal fading has been extended to Rician fading in [7]. More recently, the performance of BPSK signaling with SWC has been examined in [8] by exploiting an alternative exponential representation for the Gaussian probability integral. The authors' also derived a closed-form expression for evaluating the corresponding optimum switching threshold in Rayleigh and Nakagami-m fading channels when both diversity branches are independent and identically distributed and when the branches are of equal power and correlated.

By contrast, in this paper we derive a generic formula to study the performance of SWC for a wide range of binary and two-dimensional signal constellations in a myriad of fading environments. Different from [6]–[8], we directly determine the MGF of the resultant signal power statistic without imposing any restrictions. In fact, the signal statistics from different diversity branches may even be modeled using different families of distribution (i.e., mixed-fading). In particular, we examine the effect of power imbalance on the diversity receiver performance and

the optimal switching threshold. This is an important consideration because in practice identical fading statistics across the diversity branches are rarely available. However, all the previous theoretical studies only considered the case of identical diversity branches for analytical simplicity. Once the MGF is available, we can express the average symbol error rate (ASER) in terms of a finite-range integral involving only the MGF. Since the derivative of the MGF with respect to the switching threshold can be obtained at once, the optimum switching threshold can be readily expressed in a closed form in many instances.

The outline of this paper is as follows. In Section II, we derive the MGF of the local signal power at the output of the switched combiner, for both correlated and independent signal fading cases, taking into account power imbalance, nonidentical fading severity index and/or the mixed-fading scenario. Subsequently, a unified expression for computing the average bit or symbol error rate of different modulation formats in an arbitrary fading environment is derived. In Section III, the optimization of the SWC strategy is considered. The optimum switching threshold for both independent and correlated signal fading can be attained either in a closed form (for the identical fading statistic case) or by solving a nonlinear equation numerically (for the nonidentical fading statistics across the diversity branches). Selected numerical examples are presented in Section IV. Finally, the main points are summarized in Section V.

II. Statistical Characterization of the SNR at the Output of the SWC Combiner

Table I summarizes the instantaneous symbol error rate for a wide range of modulation schemes in an AWGN channel. Recognizing the alternative exponential form for the complementary error functions, i.e., $\mathrm{erfc}(\sqrt{\gamma}) = (2/\pi)\int_0^{\pi/2}\exp(-\gamma\csc^2\theta)d\theta$ and $\mathrm{erfc}^2(\sqrt{\gamma}) = (4/\pi)\int_0^{\pi/4}\exp(-\gamma\csc^2\theta)\,d\theta$, we can express these conditional error probabilities (for binary and two-dimension M-ary signal constellations) as a special case of the following generic form:

$$P_S(\varepsilon|\gamma) = \sum_k \int_0^{\eta_k} a_k(\theta)\exp(-\gamma b_k(\theta))d\theta \tag{1}$$

where $a_k(\theta)$ and $b_k(\theta)$ are coefficients independent of γ but may be dependent on θ. In some cases (e.g., BDPSK), $a_k(\theta) = \delta(\theta)$ where $\delta(.)$ denotes the impulse function.

The ASER in the fading channels with switched diversity can be derived by averaging the conditional error probability over the probability density function (pdf) of the SNR at the output of the switched combiner in a specified fading environment. It is more insightful if we employ the MGF approach [9]–[10] since the ASER can be expressed in terms of only the MGF of the resultant SNR. Further, closed-form formulas for the computing the optimum switching threshold can be determined in a straight-forward fashion for all common fading channels and for different modulation schemes if the diversity branches have identical fading statistics. Hence, in the following we will derive the MGF of the local power at the output of the switched combiner for both correlated and independent signal fading cases.

A. Correlated Fading and Nonidentical Diversity Branches

Similar to [4]–[7], our analysis is based on a discrete time model. The switching is performed at discrete instants of time $t = nT$, where n is an integer, and T is the interval between switching instants. The cumulative distribution function (CDF) of the resultant signal power at the output of the SWC combiner can be written as [6, eq. (4)]

$$\begin{aligned} F_{z_n}(u) &= \Pr\{z_n \le u\} \\ &= \Pr\{z_n = x_n \text{ and } x_n \le u\} + \Pr\{z_n = y_n \text{ and } y_n \le u\} \end{aligned} \tag{2}$$

where x_n and y_n denote the local powers of the signals received by the two antennas at $t = nT$, and z_n is the local signal power at the output of the switched diversity receiver at $t = nT$.

If we assume the pair of samples from each diversity branch are independent[1] (i.e., x_{n-1} and x_n are independent; y_{n-1} and y_n are independent), then (2) can be restated as

$$\begin{aligned} F_{z_n}(u) = {} & [\Pr\{\xi \le x_n \le u\} + \Pr\{x_n < \xi \text{ and } y_n \le u\}] \\ & \cdot \Pr\{z_{n-1} = x_{n-1}\} + [\Pr\{\xi \le y_n \le u\} \\ & + \Pr\{y_n < \xi \text{ and } x_n \le u\}]\Pr\{z_{n-1} = y_{n-1}\} \end{aligned} \tag{3}$$

where ξ denotes the switching threshold. In the following derivations, the time index n will be omitted for brevity. By differentiating (3) with respect to u, we obtain the following PDF of the resultant signal power z_n:

$$\begin{aligned} f_z(u) = {} & \left[f_x(u)V(u-\xi) + \int_0^{\xi} f_{x,y}(X, u)\,dX\right]\Pr\{z = x\} \\ & + \left[f_y(u)V(u-\xi) + \int_0^{\xi} f_{x,y}(u, Y)\,dY\right]\Pr\{z = y\}, \\ & u \ge 0 \end{aligned} \tag{4}$$

where $V(X) = 0$ for $X < 0$, and $V(X) = 1$, otherwise. Notations $f_x(.)$ and $F_x(.)$ correspond to the PDF and CDF of the signal power for antenna x, respectively, $f_{x,y}(.,.)$ is the joint PDF of x_n and y_n. Hence the MGF of z_n is given by

$$\begin{aligned} & \phi_z(s) \\ & = \left[\int_{\xi}^{\infty} \exp(-su) f_x(u)\,du + \int_0^{\xi} \phi_y(s, X)\,dX\right]\Pr\{z = x\} \\ & \quad + \left[\int_{\xi}^{\infty} \exp(-su) f_y(u)\,du + \int_0^{\xi} \phi_x(s, Y)\,dY\right]\Pr\{z = y\} \end{aligned} \tag{5}$$

where $\phi_x(s, Y) = \int_0^{\infty} f_{x,y}(u, Y)\exp(-su)\,du$ and $\phi_y(s, X) = \int_0^{\infty} f_{x,y}(X, u)\exp(-su)\,du$ are the marginal MGF's.

Now let us calculate the antenna selection probabilities $\Pr\{z = x\}$ and $\Pr\{z = y\}$. If both diversity branches have identical fading statistics, then each of the two antennas will

[1]This assumption is valid if T is large enough such that the fading process introduces small or no correlation in the time sequence of the samples in each branch. For small T, the justification of the final result (3) is explained in the Appendix of [6].

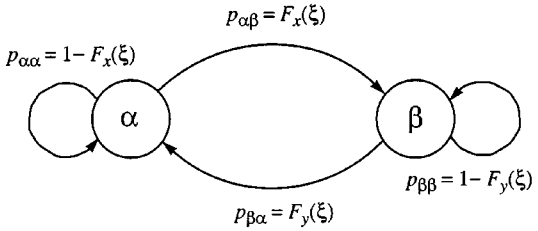

Fig. 2. A two-state Markov chain for calculating the antenna selection probabilities.

have an equal chance of being selected. However, when the sequences $\{x_n\}$ and $\{y_n\}$ are not identically distributed due to power imbalance, then the likelihood of staying in a "good" diversity branch will be higher because a branch with a higher mean received signal power will be favored most of the time. The branch selection probabilities may be computed using a two-state Markov chain shown in Fig. 2.

The states α and β correspond to the event that antenna x and antenna y is selected, respectively. The state transition probabilities, p_{ij}, are determined by the probability that the power on a specified branch is either greater or smaller than the preset threshold. The steady-state solution to this Markov chain yields the antenna selection probabilities:

$$\Pr\{z = x\} = \frac{p_{\beta\alpha}}{p_{\alpha\beta} + p_{\beta\alpha}} = \frac{F_y(\xi)}{F_x(\xi) + F_y(\xi)} \equiv A(\xi) \tag{6}$$

$$\Pr\{z = y\} = \frac{p_{\alpha\beta}}{p_{\alpha\beta} + p_{\beta\alpha}} = \frac{F_x(\xi)}{F_x(\xi) + F_y(\xi)} \equiv 1 - A(\xi). \tag{7}$$

Since $\int_\xi^\infty \exp(-su) f_x(u)\, du = \phi_x(s) - \int_0^\xi \exp(-su) f_x(u) du$ and substituting (6) and (7) into (5), we obtain a general expression for the MGF of the local signal power at the output of the switched combiner taking into account the branch correlation as well as the dissimilar fading statistics, i.e.,

$$\begin{aligned}\phi_z(s) = A(\xi)\left\{\phi_x(s) + \int_0^\xi [\phi_y(s, X) - \exp(-sX) f_x(X)]\, dX\right\} \\ + [1 - A(\xi)]\left\{\phi_y(s) + \int_0^\xi [\phi_x(s, Y) \right. \\ \left. - \exp(-sY) f_y(Y)]\, dY\right\}\end{aligned} \tag{8}$$

where $\phi_x(.)$ and $\phi_y(.)$ are the MGF of the signal power in antenna x and y, respectively (see Table II for a list of MGF's of the signal powers for several common fading channels). To the best of our knowledge, this result is new. From (1), the ABER or ASER with SWC is simply

$$P_S = \sum_k \int_0^{\eta_k} a_k(\theta) \phi_z(b_k(\theta))\, d\theta. \tag{9}$$

B. Independent Fading and Nonidentical Diversity Branches

If the antenna separation is greater than a half-wavelength, it is reasonable to assume that the two diversity branches will be independent. However, their signal strength and fading severity index may be different in an actual mobile link since the radio waves take different propagation paths and may undergo different fading before arriving at the receiver. For independent signal fading, the joint PDF is the product of the individual PDF's, and, therefore, (4) reduces to

$$\begin{aligned}f_z(u) = A(\xi)\{f_x(u)V(u - \xi) + F_x(\xi) f_y(u)\}[1 - A(\xi)] \\ \cdot\{f_y(u)V(u - \xi) + + F_y(\xi) f_x(u)\}.\end{aligned} \tag{10}$$

The MGF of z_n is

$$\begin{aligned}\phi_z(s) = A(\xi)\left\{\int_\xi^\infty \exp(-su) f_x(u) du + \phi_y(s) F_x(\xi)\right\} \\ + [1 - A(\xi)]\left\{\phi_x(s) F_y(\xi) + \int_\xi^\infty \exp(-su) f_y(u)\, du\right\}.\end{aligned} \tag{11}$$

One may also arrive at (11) directly from (8) by recognizing that $\phi_y(s, X) = f_x(X)\phi_y(s)$ and $\phi_x(s, Y) = f_y(Y)\phi_x(s)$ when the two diversity branches are statistically independent. Notice that (11) is still valid even if the received signal envelopes in different antennas are modeled by different families of the fading distribution (i.e., mixed-fading model). As before, the ASER of the SWC with uncorrelated diversity branches is given by (9). However, $\phi_z(.)$ is evaluated using (11) instead of (8).

C. Correlated Fading and Identical Diversity Branches

If x_n and y_n are identically distributed, then $f_x(.) = f_y(.)$, $\phi_x(s, .) = \phi_y(s, .)$, $F_x(.) = F_y(.)$ and $\Pr\{z = x\} = \Pr\{z = y\} = 1/2$. Owing to the symmetry, (4) reduces to [7, eq. (6)]. Similarly, the MGF of z_n illustrated in (8) may now be simplified as

$$\phi_z(s) = \phi_x(s) + \int_0^\xi [\phi_x(s, Y) - \exp(-sY) f_y(Y)]\, dY. \tag{12}$$

D. Independent Fading and Identical Diversity Branches

Following our treatment in Section II-C, it is straight-forward to show that (4) reduces to [7, eq. (7)] for the independent and identically distributed diversity branches. Hence the MGF of the resultant signal power is given by

$$\phi_z(s) = \phi_x(s) F_x(\xi) + \int_\xi^\infty \exp(-su) f_x(u)\, du. \tag{13}$$

III. Optimization of the SWC Strategy

As discussed in [8], if the switching threshold ξ is set to be very large, then there will be constant switching between the two antennas because the probability of the received signal exceeding ξ will be small. In this case, the performance of SWC will be equivalent to the performance of a diversity branch selected in random, which resembles the behavior for the no diversity case. On the other extreme (i.e., the value of ξ is set to be very small), the SWC combiner will be stuck in one of the diversity branches because the likelihood of the received signal power staying above the specified threshold increases. Once again, the performance of the SWC will be close to the single diversity branch case. It is evident that the performance

TABLE II
PDF AND MGF OF SIGNAL POWER FOR SEVERAL COMMON FADING FORMATS

Channel Model	PDF and MGF of signal power X
Rayleigh	PDF: $f_x(X) = \frac{1}{\Omega}\exp\left(\frac{-X}{\Omega}\right)$ where $\Omega = E[X]$
	MGF: $\phi_x(s) = \frac{1}{1+s\Omega}$
Rician ($K \geq 0$)	PDF: $f_x(X) = \frac{1+K}{\Omega}\exp\left(-K-\frac{(1+K)X}{\Omega}\right)I_0\left(2\sqrt{\frac{K(K+1)X}{\Omega}}\right)$
	MGF: $\phi_x(s) = \frac{1+K}{1+K+s\Omega}\exp\left(\frac{-Ks\Omega}{1+K+s\Omega}\right)$
Nakagami-q ($-1 \leq b \leq 1$)	PDF: $f_x(X) = \frac{1}{\Omega\sqrt{1-b^2}}\exp\left(\frac{-X}{[1-b^2]\Omega}\right)I_0\left(\frac{bX}{[1-b^2]\Omega}\right)$
	MGF: $\phi_x(s) = \frac{1}{\sqrt{[s\Omega(1+b)+1][s\Omega(1-b)+1]}}$
Nakagami-m ($m \geq 0.5$)	PDF: $f_x(X) = \left(\frac{m}{\Omega}\right)^m \frac{X^{m-1}}{\Gamma(m)}\exp\left(\frac{-mX}{\Omega}\right)$
	MGF: $\phi_x(s) = \left(\frac{m}{m+s\Omega}\right)^m$
Correlated Nakagami-m with identical mean signal strength (i.e., $\Omega_x = \Omega_y$)	PDF: $f_{x,y}(X,Y) = \frac{(m/\Omega)^{m+1}}{\Gamma(m)[1-\rho]\rho^{(m-1)/2}}(XY)^{\frac{m-1}{2}}\exp\left(\frac{-m(X+Y)}{\Omega[1-\rho]}\right)I_{m-1}\left(\frac{2m\sqrt{\rho XY}}{\Omega[1-\rho]}\right)$
	MGF: $\phi_x(s,Y) = \left(\frac{m}{\Omega}\right)^m \frac{Y^{m-1}}{\Gamma(m)[1+s\Omega[1-\rho]/m]^m}\exp\left\{\frac{-mY}{\Omega}\left[\frac{m+s\Omega}{m+s\Omega(1-\rho)}\right]\right\}$ where ρ is the power correlation coefficient.
Correlated Nakagami-m with power imbalance	PDF: $f_{x,y}(X,Y) = \frac{[m/\sqrt{\Omega_x\Omega_y}]^{m+1}}{\Gamma(m)[1-\rho]\rho^{(m-1)/2}}(XY)^{\frac{m-1}{2}}\exp\left(\frac{-m(X+Y)}{\sqrt{\Omega_x\Omega_y}[1-\rho]}\right)I_{m-1}\left(\frac{2m\sqrt{\rho XY}}{\sqrt{\Omega_x\Omega_y}[1-\rho]}\right)$
	MGF: $\phi_x(s,Y) = \frac{1}{\Gamma(m)}\left[\frac{m^2}{\Omega_y(m+s(1-\rho)\Omega_x)}\right]^m Y^{m-1}\exp\left\{\frac{-mY}{\Omega_y}\left[\frac{m+s\Omega_x}{m+s\Omega_x(1-\rho)}\right]\right\}$

of this switched diversity strategy is dependent on the selection of the switching threshold, and proper choice of ξ will minimize the average error probability. Hence in this section, we will derive analytical expressions that will allow us to compute the optimum switching threshold (in the minimum error rate sense) either in a closed form (for identical fading statistics) or numerically (for nonidentical fading statistics) for a broad class of digital modulation formats in arbitrary fading environments.

A. Correlated Fading and Nonidentical Diversity Branches

Differentiating (8) with respect to ξ, we get

$$\begin{aligned}\frac{\partial}{\partial\xi}\phi_z(s) &= A(\xi)[\phi_y(s,\xi)-\exp(-s\xi)f_x(\xi)]\\ &\quad+[1-A(\xi)][\phi_x(s,\xi)-\exp(-s\xi)f_y(\xi)]\\ &\quad+B(\xi)\left[\phi_x(s)-\phi_y(s)+\int_0^{\xi}[\phi_y(s,u)-\phi_x(s,u)\right.\\ &\qquad\left.+\{f_y(u)-f_x(u)\}\exp(-su)]\,du\right] \qquad (14)\end{aligned}$$

where $A(\xi)$ is defined in (6) and

$$B(\xi) = \frac{\partial}{\partial\xi}A(\xi) = \frac{F_x(\xi)f_y(\xi)-F_y(\xi)f_x(\xi)}{[F_x(\xi)+F_y(\xi)]^2}. \qquad (15)$$

Now our task is to find the optimum ξ^* that minimizes the ASER. This value can be determined by solving $\partial P_S/\partial\xi = 0$ for ξ. By differentiating (9) under the integral sign, and exploiting the results of (14), we have

$$\begin{aligned}\frac{dP_S}{d\xi} &= \sum_k\int_0^{\eta_k} a_k(\theta)[A(\xi)\phi_y(b_k(\theta),\xi)+\{1-A(\xi)\}\phi_x(b_k(\theta),\xi)]d\theta\\ &\quad+B(\xi)\sum_k\int_0^{\eta_k}a_k(\theta)\left[\int_0^{\xi}[\phi_y(s,u)-\phi_x(s,u)\right.\\ &\quad\left.+\{f_y(u)-f_x(u)\}\exp(-su)]du\right]d\theta+B(\xi)\\ &\quad[P_S^{(x)}-P_S^{(y)}]-P_S(\varepsilon|\xi)[A(\xi)f_x(\xi)+\{1-A(\xi)\}f_y(\xi)] \qquad (16)\end{aligned}$$

where notation $P_S^{(x)}$ and $P_S^{(y)}$ correspond to the ASER of the diversity branch x [i.e., obtained by replacing $\phi_z(s)$ in (9) with $\phi_x(s)$] and y, respectively. For this general case, no closed-form solution for ξ^* exists. Hence, this value will be determined numerically.

B. Independent Fading and Nonidentical Diversity Branches

If the diversity branches are assumed to be statistically independent, then we may replace the marginal MGF's in (16) with $\phi_y(s, u) = f_x(u)\phi_y(s)$ and $\phi_x(s, u) = f_y(u)\phi_x(s)$. Then it can be easily shown that the optimal threshold is obtained by solving the following expression:

$$\begin{aligned} &A(\xi)f_x(\xi)P_S^{(y)} + \{1 - A(\xi)\}f_y(\xi)P_S^{(x)} + B(\xi) \\ &\quad \cdot [F_x(\xi)P_S^{(y)} - F_y(\xi)P_S^{(x)}] + B(\xi)\sum_k \int_0^{\eta_k} a_k(\theta) \\ &\quad \cdot \left[\int_\xi^\infty [\{f_y(u) - f_x(u)\}\exp(-su)]\,du\right] d\theta \\ &\quad - P_S(\varepsilon|\xi)[A(\xi)f_x(\xi) + \{1 - A(\xi)\}f_y(\xi)] = 0. \end{aligned} \quad (17)$$

C. Independent Fading and Identical Diversity Branches

If both the diversity branches are assumed to be independent and identically distributed, then the PDF, CDF, and MGF of x_n and y_n are interchangeable. Moreover, $A(\xi) = 1/2$ and $B(\xi) = 0$. In this case, (17) reduces to

$$P_S(\varepsilon|\xi) = P_S^{(x)} = P_S^{(y)} \quad (18)$$

where $P_S^{(x)}$ or $P_S^{(y)}$ corresponds to the ASER without diversity reception. Next we will identify three special cases of the conditional error probability $P_S(\varepsilon|\gamma)$ which lend themselves to closed-form formulas for the calculation of ξ^* in all common fading environments.

1) Exponential Form: $P_S(\varepsilon|\gamma) = a\exp(-b\gamma)$: The instantaneous BER of some noncoherent binary modulation schemes (e.g., DPSK and NCFSK) can be expressed in an exponential form. Then $P_S = a\phi_z(b)$ for the switched diversity receiver, and their corresponding optimum switching threshold is [directly from (18)]

$$\xi^* = \frac{-1}{b}\ln\left(\frac{P_S^{(x)}}{a}\right) = \frac{-\ln(\phi_x(b))}{b}. \quad (19)$$

Substituting $b = 1/2$ and using the appropriate expression for $\phi_x(.)$, we arrive at the previous expressions for the optimum threshold of NCFSK in Nakagami-m [6, eq. (14)] and Rician [7, eq. (12)] fading channels, respectively.

2) 1-D Complementary Error Function: $P_S(\varepsilon|\gamma) = a\,\mathrm{erfc}(\sqrt{b\gamma}) = (2a/\pi)\int_0^{\pi/2}\exp(-\gamma b\csc^2\theta)\,d\theta$: The ASER of some coherent binary modulation schemes (e.g., CPSK and CFSK) with SWC is given by $P_S = (2a/\pi)\int_0^{\pi/2}\phi_z(b\csc^2\theta)d\theta$. Using (18), we get

$$\begin{aligned} \xi^* &= \frac{1}{b}(\mathrm{erfcinv}[P_S^{(x)}/a])^2 \\ &= \frac{1}{b}\left(\mathrm{erfcinv}\left[\frac{2}{\pi}\int_0^{\pi/2}\phi_x(b\,\csc^2\theta)d\theta\right]\right)^2 \end{aligned} \quad (20)$$

where $\mathrm{erfcinv}(.)$ denotes the inverse of the complementary error function.

3) 1-D and 2-D Complementary Error Functions: $P_S(\varepsilon|\gamma) = a\,\mathrm{erfc}(\sqrt{b\gamma}) - c\,\mathrm{erfc}^2(\sqrt{b\gamma})$: The ASER for square QAM, QPSK and coherent detection of differentially encoded PSK with SWC is given by $P_S = (2a/\pi)\int_0^{\pi/2}\phi_z(b\csc^2\theta)\,d\theta - (4c/\pi)\int_0^{\pi/4}\phi_z(b\csc^2\theta)\,d\theta$. By solving the quadratic $c\,\mathrm{erfc}^2(\sqrt{b\xi}) - a\,\mathrm{erfc}(\sqrt{b\xi}) + P_S^{(x)} = 0$ for ξ [i.e., see (18)], we obtain a closed-form expression for the optimal switching threshold

$$\xi^* = \frac{1}{b}\left\{\mathrm{erfcinv}\left[\frac{a - \sqrt{a^2 - 4cP_S^{(x)}}}{2c}\right]\right\}^2. \quad (21)$$

For example, the optimal switching threshold for the QPSK or the 4-QAM modulation scheme is given by

$$\xi^* = \left(\mathrm{erfcinv}\left(2\left[1 - \sqrt{1 - P_S^{(x)}}\right]\right)\right)^2 \quad (22)$$

where

$$P_S^{(x)} = (2/\pi)\int_0^{\pi/2}\phi_x(\csc^2\theta)d\theta - (1/\pi)\int_0^{\pi/4}\phi_x(\csc^2\theta)d\theta.$$

D. Correlated Fading and Identical Diversity Branches

If the assumption of branch independence is slightly relaxed, then we may only get the optimal ξ in a closed form for the exponential form of $P_S(\varepsilon|\gamma)$ in correlated Rayleigh and/or correlated Nakagami-m fading channels. Following our treatment for the independent signal fading, the optimal switching threshold for the differentially coherent or the noncoherent binary modulation format is obtained by solving $(\partial/\partial\xi)\phi_z(b) = 0$ for ξ:

$$\phi_x(b, \xi) - f_x(\xi)\exp(-b\xi) = 0. \quad (23)$$

Substituting the marginal MGF for the correlated Nakagami-m fading channel with identical mean received signal strength (see Table II) in (23), we get

$$\xi^* = m\left[\frac{m + b\Omega(1-\rho)}{b(1-\rho)(m+b\Omega}\right]\ln\left(1 + \frac{b\Omega(1-\rho)}{m}\right) \quad (24)$$

which is a generalization of Eq. (24) in [6] for the differentially coherent binary signaling and for arbitrary m values. By setting the power correlation coefficient $\rho = 0$, (24) reduces to (19). For other modulation formats listed in Table I, ξ^* is given by the unique real positive root of (25), which will be determined numerically according to

$$\sum_k \int_0^{\eta_k} a_k(\theta)\phi_x(b_k(\theta), \xi)\,d\theta - f_x(\xi)P_s(\varepsilon|\xi) = 0. \quad (25)$$

IV. Numerical Results

In this section, we provide selected numerical examples to show the generality of the new results derived in this paper. The performances of SWC (with optimum switching thresholds) for different M-ary signaling constellations in Rayleigh and Rician fading channels are shown in Fig. 3. For the Rician fading

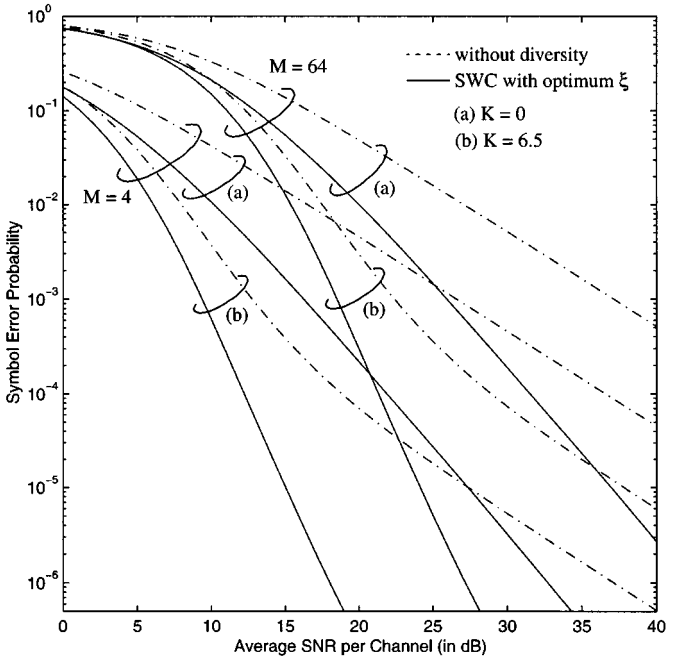

Fig. 3. Performance of MQAM with SWC in Rayleigh and Rician fading channels.

channel, the CDF of signal power (for a single branch) is given by

$$F_i(\xi) = 1 - Q\left(\sqrt{2K_i},\ \sqrt{2(1+K_i)\xi/\Omega_i}\right) \tag{26}$$

and

$$\begin{aligned}\lambda_i(\xi, s) &= \int_{\xi}^{\infty} \exp(-su) f_i(u)du \\ &= \frac{1+K_i}{s\Omega_i + K_i + 1} \exp\left(\frac{-sK_i\Omega_i}{s\Omega_i + K_i + 1}\right) \\ &\quad \times Q\left(\sqrt{\frac{2K_i(K_i+1)}{s\Omega_i + K_i + 1}}, \sqrt{\frac{2(s\Omega_i + K_i + 1)\xi}{\Omega_i}}\right)\end{aligned} \tag{27}$$

where $i \in \{x, y\}$, and $Q(\sqrt{2a}, \sqrt{2b}) = \int_b^{\infty} \exp(-t - a) I_0(2\sqrt{at})\, dt$ is the Marcum-Q function. If the received signal envelopes from the two antennas are assumed to be independent and identically distributed, then $\Omega_i = \Omega$ and $K_i = K$. Substituting (26) and (27) into (13), we get a closed-form expression for $\phi_z(.)$, i.e.,

$$\begin{aligned}\phi_z(s) &= \frac{1+K}{s\Omega + K + 1} \exp\left(\frac{-sK\Omega}{s\Omega + K + 1}\right) \\ &\quad \times \left[1 - Q\left(\sqrt{2K}, \sqrt{\frac{2(1+K)\xi^*}{\Omega}}\right)\right. \\ &\quad \left. + Q\left(\sqrt{\frac{2K(K+1)}{s\Omega + K + 1}}, \sqrt{\frac{2(s\Omega + K + 1)\xi^*}{\Omega}}\right)\right]\end{aligned} \tag{28}$$

and the optimal threshold $\xi*$ is calculated using (21). For Rayleigh fading, (28) reduces to

$$\phi_z(s) = \frac{1}{s\Omega + 1}\left[1 - \exp(-\xi^*/\Omega) + \exp(-(s\Omega + 1)\xi^*/\Omega)\right] \tag{29}$$

since $Q(0, \beta) = \exp(-\beta^2/2)$.

From Fig. 3, it is apparent that the diversity reception is a simple yet powerful technique for mitigating the effect of deep fades experienced in wireless channels. For instance, the dual-branch SWC system can reduce the penalty in the required SNR to achieve an error rate of $P_S = 10^{-3}$ for the 64-QAM by approximately 11 dB in a Rayleigh fading channel with respect to the no diversity case. The diversity advantage is greater for a larger alphabet size and in a poorer channel condition (i.e., as $K \to 0$), as anticipated.

In Fig. 4, we examine the effect of power imbalance on the performance of BDPSK with SWC on a Rayleigh fading channel. Using (11) and (27), we can express the ABER as

$$\begin{aligned}P_S &= \frac{1}{2}\phi_z(1) \\ &= \frac{A(\xi^*)}{2}\left[\frac{F_x(\xi^*)}{\Omega_y + 1} + \lambda_x(\xi^*, 1)\right] \\ &\quad + \frac{1 - A(\xi^*)}{2}\left[\frac{F_y(\xi^*)}{\Omega_x + 1} + \lambda_y(\xi^*, 1)\right]\end{aligned} \tag{30}$$

where

$$F_i(\xi) = 1 - \exp(-\xi/\Omega_i) \tag{31}$$

and

$$\lambda_i(\xi, 1) = \frac{1}{\Omega_i + 1} \exp\left(\frac{-\xi(\Omega_i + 1)}{\Omega_i}\right) \tag{32}$$

are obtained by setting $K = 0$ and $s = 1$ in (26) and (27). The optimum switching threshold is given by the real positive root of (33)

$$\begin{aligned}&A(\xi) f_x(\xi)\left[\frac{1}{\Omega_y + 1} - \exp(-\xi)\right] \\ &\quad + [1 - A(\xi)] f_y(\xi)\left[\frac{1}{\Omega_x + 1} - \exp(-\xi)\right] \\ &\quad + B(\xi)\left[\frac{F_x(\xi)}{\Omega_y + 1} - \frac{F_y(\xi)}{\Omega_x + 1} + \lambda_x(\xi, 1) - \lambda_y(\xi, 1)\right] = 0\end{aligned} \tag{33}$$

where $A(\xi)$ and $B(\xi)$ are defined in (6) and (15), respectively.

In Fig. 4(a), the optimum switching threshold is plotted as a function Ω_x of for the following four cases: 1) $\Omega_y = \Omega_x$; 2) $\Omega_y = 2\Omega_x$; 3) $\Omega_y = 5\Omega_x$; and 4) $\Omega_x = 10\Omega_y$. We find that the optimum threshold (corresponding to the solid-line curves) decreases rapidly as the ratio Ω_y/Ω_x decreases. This trend can be explained by noting that when the power imbalance between the two diversity branches increases, then a lower threshold level is desirable so that the switched combiner will have an increased

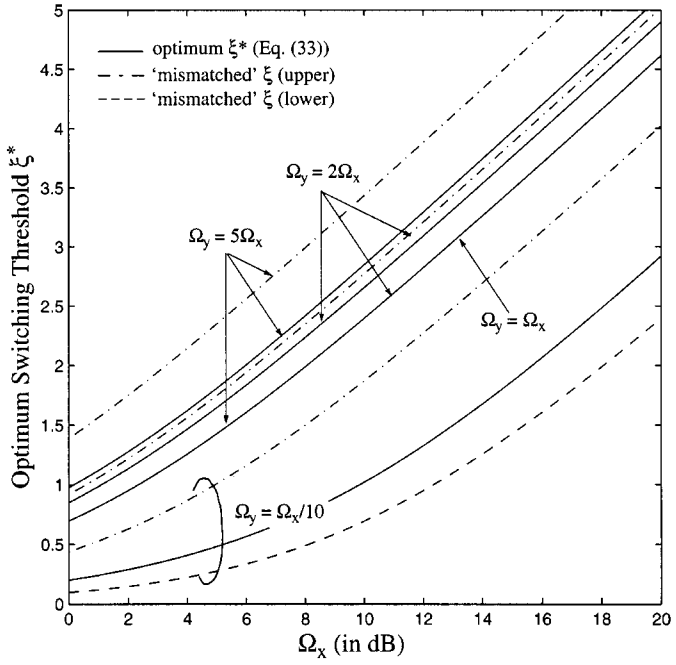

(a)

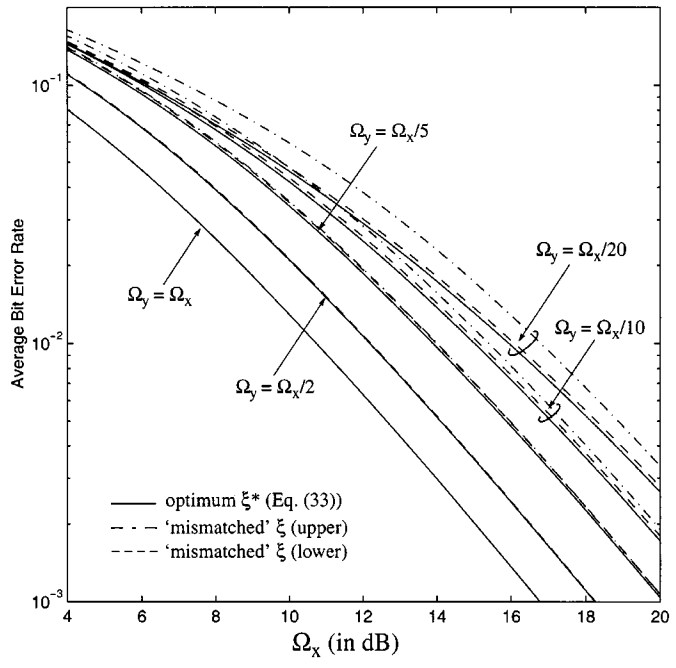

(b)

Fig. 4. (a) Effect of power imbalance on the optimal switching threshold for BDPSK in a Rayleigh fading channel. (b) Sensitivity of the average bit error rate performance of BDPSK to the mismatch in the optimal switching threshold on a Rayleigh fading channel.

likelihood of choosing and staying in a "good" branch. Furthermore, a very large value for ξ only results in performance degradation due to bad switchings.

The optimal switching threshold for the independent and identically distributed (i.i.d.) case can be determined in closed form for three different forms of conditional error probability, as derived in Section III-C. For these cases, is also desirable if we can provide an estimate of ξ^* in a closed form for the nonidentical fading statistics situation. Exploiting the trends from Fig. 4(a) and using (19), it is possible to bound the optimal threshold for the exponential form as

$$-\ln[\phi_{AL}(b)]/b \le \xi^* \le -\ln[\phi_{AU}(b)]/b \tag{34}$$

where $\phi_{AL}(.) = \max\{\phi_x(.), \phi_y(.)\}$ (which corresponds to the MGF of the "weaker" branch), and the mean signal power used in $\phi_{AU}(.)$ is the average of signal power received from the two diversity branches, i.e., $\Omega_{AU} = (\Omega_x + \Omega_y)/2$. These bound are also plotted in Fig. 4(a). All the three curves coincide when $\Omega_y = \Omega_x$ and the optimal threshold is much closer to the upper limit if $0.25 < \Omega_y/\Omega_x < 4$, and the lower limit otherwise. It is also noted that the lower limit of the optimal threshold for case ii) and iii) is given by ξ^* of the i.i.d. case. We have also verified that the optimal threshold obtained using (19) and (33) are identical for case i). Expressions similar to (34) can be easily derived for $P_S(\varepsilon|\gamma)$ in the form of a 1-D complementary error function or a combination of 1-D and 2-D complementary error functions.

In Fig. 4(b), we investigate the sensitivity of the ABER to "mismatch" in the switching threshold level. The solid and the dashed or the dash-dot curves correspond to the optimal threshold [calculated using (33)] and the threshold level predicted using (34), respectively. While there can be a noticeable difference in the switching threshold levels [e.g., see the curves corresponding to $\Omega_y = 2\Omega_x$ and $\Omega_y = 5\Omega_x$ in Fig. 4(a)], the ABER performance appears to be not too sensitive to this variation. In fact, we find that the lower bound given in (34) can be viewed as a good coarse approximation of ξ^*, and therefore is attractive for rapid computation of the ASER or ABER. The discrepancy between the true and approximate ABER curves becomes appreciable only when the mean received signal power imbalance is very large.

Subsequently in Fig. 5, we study the effect of dissimilar fading severity index $(K_y \neq K_x)$ on the performance of 8-PSK with SWC. The corresponding ASER of MPSK can be easily shown to be

$$P_S = \int_0^{\pi - \pi/M} \phi_z\left(\frac{\sin^2(\pi/M)\log_2 M}{\sin^2\theta}\right) d\theta \tag{35}$$

where $\phi_z(.)$ is obtained by substituting (26) and (27) into (11), and then setting $\Omega_i = \Omega$. From Fig. 5, we can conclude that the optimal switching threshold and the ASER are not severely affected by unequal fading index unless the perturbation is very large. Once again the optimum switching threshold point shifts to the left as the discrepancy between K_x and K_y gets larger. Now look at the $P_S^{(x)}$, $P_S^{(y)}$ and the SWC curves corresponding to case (c) with $\Omega = 10$ dB. While the SWC will always perform better than any of the two identical diversity branches for the entire region of ξ [see the curves for case (a)], this may not be necessarily true if the branch statistics are not identical. If ξ is chosen to be very large, the performance of SWC will be dictated by the average performance of the two diversity branches (due to the random switching). On the other extreme (i.e., ξ is set to a very small value), the SWC closely resembles the performance of the branch with better statistics. For the cases (b) and (c), we observe that the performance of SWC is actually slightly worse than $P_S^{(x)}$ as $\xi \to 0$. This is because there is always a finite probability that the "weaker" branch will be selected and

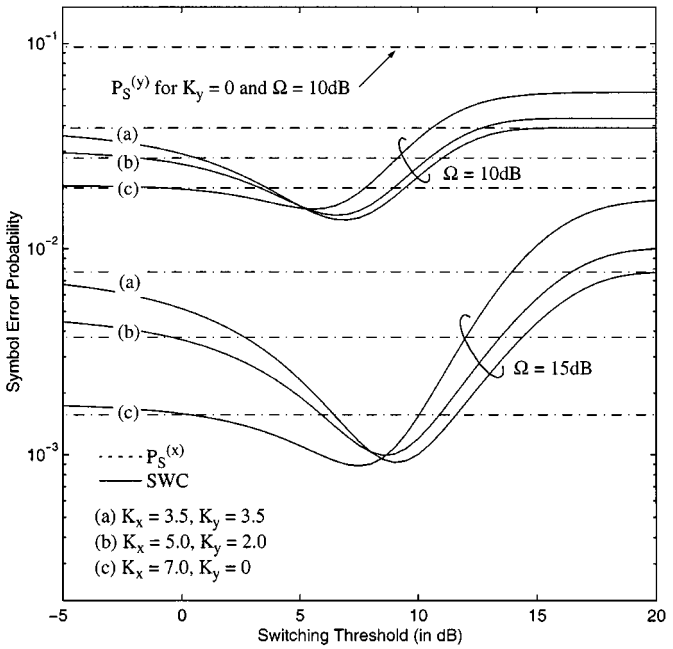

Fig. 5. Effects of nonidentical fading severity index on the optimal switching threshold level and the SER performance of an 8-PSK signaling scheme.

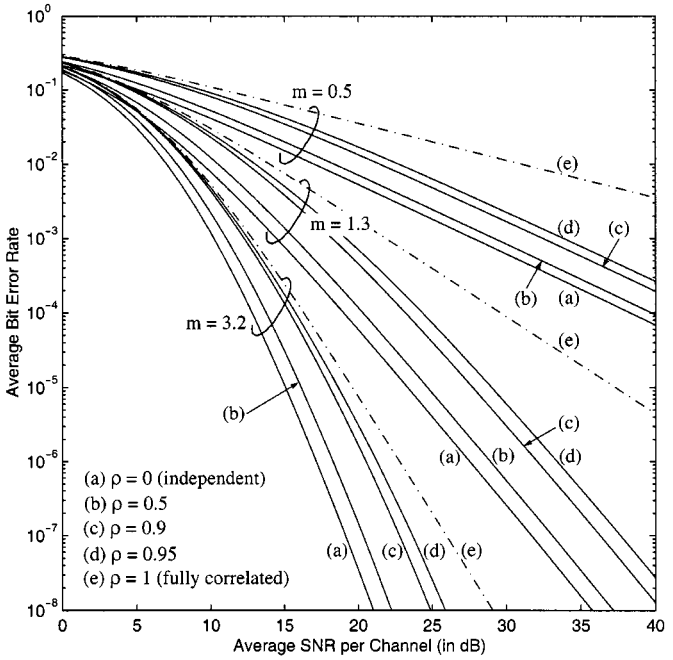

Fig. 6. Effect of branch correlations on the attainable switched diversity gain for BDPSK modulation format in Nakagami-m fading channels.

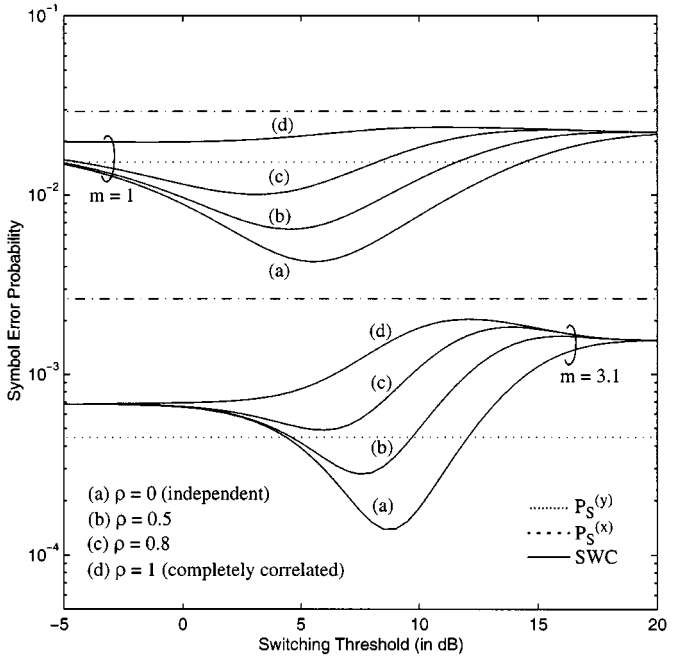

(a)

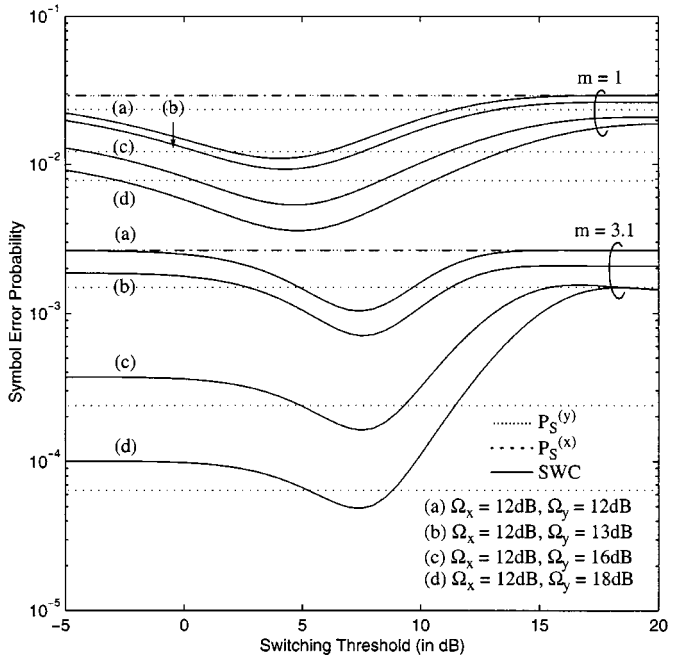

(b)

Fig. 7. (a) Sensitivity of the ASER of $\pi/4$-DQPSK and the optimal switching threshold level to the branch correlations in the presence of dissimilar mean received signal strengths $\Omega_x = 12$ dB and $\Omega_y = 15$ dB.

the averaging of the error performance contributes to this phenomena. Comparison between the curves for case (b) and case (c) reveal that this gap actually diminishes as the difference between the fading severity indexes gets larger, as anticipated.

In Fig. 6, we quantify the switched diversity receiver performance degradation due to branch correlation for the BDPSK modulation scheme. We have assumed both the diversity branches have equal mean received signal strengths to isolate its effect on the ABER performance. For the correlated Nakagami-m channel, it is more convenient to rewrite (12) as (36) since both the integrals can be directly expressed in terms of the incomplete Euler integrals as

$$\begin{aligned}\phi_z(s) &= \int_{\xi}^{\infty} \exp(-sY) f_y(Y) dY + \int_0^{\xi} \phi_x(s, Y)\, dY \\ &= \frac{1}{\Gamma(m)} \left(\frac{m}{m+s\Omega}\right)^m \{\Gamma[m, \xi(s+m/\Omega)] \\ &\quad \cdot + \gamma\left[m, \frac{\xi(s+m/\Omega)}{1+s\Omega(1-\rho)/m}\right]\} \end{aligned} \tag{36}$$

$$\phi_z(s) = \frac{A(\xi)\Gamma[m,\, \xi(s+m/\Omega_x)] + [1-A(\xi)]\gamma\left[m,\, \dfrac{m\xi(m+s\Omega_x)}{\Omega_y(m+s\Omega_x(1-\rho))}\right]}{\Gamma(m)(1+s\Omega_x/m)^m} + \frac{[1-A(\xi)]\Gamma[m,\xi(s+m/\Omega_y)] + A(\xi)\gamma\left[m,\, \dfrac{m\xi(m+s\Omega_y)}{\Omega_x(m+s\Omega_y(1-\rho))}\right]}{\Gamma(m)(1+s\Omega_y/m)^m} \tag{38}$$

where $\gamma(a,\, x) = \int_0^x \exp(-t)t^{a-1}dt$, $a > 0$ is the incomplete Gamma function, and its companion is defined as $\Gamma(a,\, x) = \Gamma(a) - \gamma(a,\, x) = \int_x^\infty \exp(-t)t^{a-1}\,dt$ (known as the complementary incomplete Gamma function) [16]. Now substituting (24) and (36) into (9), we get a simple closed-form expression for calculating the ABER of BDPSK with the optimal switching threshold, namely $P_S = 0.5\phi_z(1)$. When the power correlation coefficient ρ increases, the switched diversity receiver performance degrades due to the increased likelihood of simultaneous deep signal fades at the branch inputs. From Fig. 6, we can also conclude that the low branch correlation has negligible effect on the achievable diversity gain and the average SER performance does not seriously deteriorate unless $\rho \gg 0.5$. Even with a high value of correlation a significant diversity improvement can still be realized, particularly in channels that experience severe deep fades. For instance, the diversity gain in a Nakagami-m fading channel with fading index $m = 1.3$ is more than 9 dB and 6 dB at $P_S = 10^{-4}$ for $\rho = 0.5$ and $\rho = 0.9$, respectively. When the two branches are completely correlated, the ABER curve for SWC collapses to the no diversity case as expected.

Finally in Fig. 7, the ASER of $\pi/4$-DQPSK are plotted as a function of switching threshold for the correlated Rayleigh and Nakagami-m fading channels with nonidentical mean received signal strength. Using (8) and (9), and then following the development of (36), we can express the corresponding exact ASER in terms of a finite-range integral

$$P_S = \frac{1}{2\pi}\int_0^\pi \frac{\phi_z\left(2-\sqrt{2}\,\cos\theta\right)}{\sqrt{2}-\cos\theta}d\theta = \frac{1}{2\pi}\int_0^\pi \phi_z\left(\frac{2}{2-\sqrt{2}\cos\theta}\right)d\theta \tag{37}$$

where $\phi_z(.)$ is now given by (38) at the top of the page and $A(\xi)$ is evaluated using (6) with $F_i(\xi) = \gamma(m,\, m\xi/\Omega_i)/\Gamma(m)$ for $i \in \{x,\, y\}$. The second integral in (37) can be obtained from the first integral through geometric relations (see in [12, eq. (10)]). While ξ^* increases as the channel condition improves [i.e., the optimum threshold level in Fig. 7(a) and (b) shifts to the right of the x-axis as m increases], it declines as ρ gets larger. Fig. 7(a) also reveals that high branch correlation levels can seriously deteriorate the ASER performance in the presence of power imbalance, specifically if the fading severity index is large. For instance, the SWC exhibits an inferior performance compared to the diversity branch y alone even at the optimum switching threshold when $\rho = 0.8$, $\Omega_x = 12$ dB, and $\Omega_y = 15$ dB.

It is also interesting to note that the optimal switching threshold remains almost unaffected despite a large deviation in the mean received signal strength across the diversity branches [see Fig. 7(b)]. This in turn suggests that we can estimate ξ^* for the power imbalance case by computing the optimal threshold for the identical branches with $\Omega = \min\{\Omega_x,\, \Omega_y\}$. This observation also validates the usefulness of the idea established in (34) for rapid calculation of the approximate ASER for several modulation formats (i.e., if a closed-form formula for computing ξ^* is available) when the restriction of identical fading statistics is relaxed.

V. Conclusions

This paper presents a concise, unified approach for evaluating switched diversity receiver performance for a wide range of modulation formats and fading environments. Recent studies [8]–[11], [13]–[15] have shown that the MGF enables rapid computation of the ABER and ASER. Therefore, this paper derives the MGF of the SWC output directly. As well, the derivative of the MGF follows at once, which is used to determine the optimal (in the minimum error rate sense) switching threshold. Commonly used MGF's and the conditional SER formulas are tabulated for the use with our generic expressions. Results of [6]–[8] are presented as special cases of our analysis. Closed-form expressions for the optimal switching threshold are derived for three generic forms of conditional SER probability by assuming identical fading statistics across the statistically independent diversity branches. When the effect of branch correlation is taken into account, a closed-form formula for the optimal switching threshold is only available for the exponential form of conditional error probability in Rayleigh and Nakagami-m fading channels with equal mean received signal strengths.

References

[1] A. J. Rustako, Jr., Y. S. Yeh, and R. R. Murray, "Performance of feedback and switch space diversity 900 MHz FM mobile radio systems with Rayleigh fading," *IEEE Trans. Commun.*, vol. 21, pp. 1257–1268, Nov. 1993.

[2] W. E. Shortall, "A switched diversity receiving system for mobile radio," *IEEE Trans. Commun.*, vol. 21, pp. 1269–1275, Nov. 1973.

[3] F. Adachi, T. Hattori, K. Hirade, and T. Kamata, "A periodic switching diversity technique for a digital FM land mobile radio," *IEEE Trans. Veh. Technol.*, vol. 27, pp. 211–219, Nov. 1978.

[4] M. A. Blanco and K. J. Zdunek, "Performance and optimization of switched diversity systems for detection of signals with Rayleigh fading," *IEEE Trans. Commun.*, vol. 27, pp. 1887–1895, Dec. 1979.

[5] M. Blanco, "Diversity receiver performance in Nakagami fading," in *Proc. 1983 IEEE Southeastern Conf.*, Orlando, pp. 529–532.

[6] A. Abu-Dayya and N. C. Beaulieu, "Analysis of switched diversity system on generalized-fading channels," *IEEE Trans. Commun.*, vol. 42, pp. 2959–2966, Nov. 1994.

[7] ——, "Switched diversity on microcellular Rician channels," *IEEE Trans. Veh. Technol.*, vol. 43, pp. 970–976, Nov. 1994.

[8] M. K. Simon and M. S. Alouini, "Tutorial notes TU 08: A unified approach to the error probability analysis of digital communication over generalized fading channels," in *IEEE Global Telecommunications Conf.*, Sydney, Nov. 8–12, 1998.

[9] C. Tellambura, A. J. Mueller, and V. K. Bhargava, "Analysis of M-ary phase-shift-keying with diversity reception for land-mobile satellite channels," *IEEE Trans. Vehicular Technology*, vol. 46, pp. 910–922, Nov. 1997.
[10] C. Tellambura and V. K. Bhargava, "Unified error analysis of DQPSK in fading channels," *Electron. Lett.*, vol. 30, no. 25, pp. 2110–2111, Dec. 1994.
[11] A. Annamalai, C. Tellambura, and V. K. Bhargava, "Unified analysis of MPSK and MDPSK with diversity reception in different fading environments," *Electron. Lett.*, vol. 34, no. 16, pp. 1564–1565, Aug. 1998.
[12] R. F. Pawula, "A new formula for MDPSK symbol error probability," *IEEE Commun. Lett.*, vol. 2, pp. 271–272, Oct. 1998.
[13] X. Dong, N. C. Beaulieu, and P. H. Wittke, "Two dimensional signal constellations for fading channels," in *IEEE GLOBECOM, Communication Theory Mini Conf,*, Nov. 8–12, 1998, pp. 22–27.
[14] M. Simon and M. Alouini, "A unified approach to performance analysis of digital communication over generalized fading channels," *Proc. IEEE*, vol. 86, pp. 1860–1877, Sept. 1998.
[15] M. Alouini and A. Goldsmith, "A unified approach for calculating error rates of linearly modulated signals over generalized fading channels," in *Proc. ICC'98*, Atlanta, GA, June 1998, pp. 459–464.
[16] I. S. Gradshteyn and I. M. Ryzhik, *Table of Integrals, Series and Products*. New York: Academic, 1995.
[17] X. Dong, N. C. Beaulieu, and P. H. Wittke, "Signal constellations for fading channels," *IEEE Trans. Commun,*, vol. 47, pp. 703–714, May 1999.

Chinthananda Tellambura (M'97) received the B.Sc. degree (with honors) from the University of Moratuwa, Sri Lanka, in 1986, the M.Sc. degree in electronics from the King's College, U.K., in 1988, and the Ph.D. degree in electrical engineering from the University of Victoria, Canada, in 1993.

He was a post-doctoral research fellow with the University of Victoria and the University of Bradford. Currently, he is a Senior Lecturer at Monash University, Clayton, Australia.

Dr. Tellambura is an Editor for the IEEE TRANSACTIONS ON COMMUNICATIONS and the IEEE JOURNAL ON SELECTED AREAS IN COMMUNICATIONS (Wireless Communications Series). His research interests include coding, communication theory, modulation, equalization and wireless communications.

A. Annamalai (M'94) received the B.Eng. degree (with the highest distinction) from the University of Science of Malaysia in 1993, and the M.A.Sc. and Ph.D. degrees from the University of Victoria, Canada, in 1997 and 1999, respectively, all in electrical and computer engineering.

He was an RF design engineer with Motorola Inc. from 1993 to 1995. Currently, he is with the Bradley Department of Electrical and Computer Engineering of Virginia Tech as an Assistant Professor. His research interests are in high-speed data transmission over wireless links, adaptive modulation and coding, smart antenna, OFDM and wireless communication theory.

Dr. Annamalai was the recipient of the 2000 NSERC Doctoral Prize, 2000 CAGS/UMI Distinguished Dissertation Award in the Natural Sciences, Medicine and Engineering and the 2001 IEEE Leon K. Kirchmayer Prize Paper Award for his work on diversity systems. He is an Editor for the IEEE JOURNAL ON SELECTED AREAS IN COMMUNICATIONS (Wireless Series), an Associate Editor for the IEEE COMMUNICATIONS LETTERS and is the Technical Program Chair of the IEEE VTC2002 (Fall).

Vijay K. Bhargava (S'70–M'74–SM'82–F'92) received the B.Sc., M.Sc., and Ph.D. degrees from Queen's University, Kingston, Canada, in 1970, 1972, and 1974, respectively.

He is currently is a Professor of Electrical and Computer Engineering at the University of Victori and is currently spending a sabbatical year at the Hong Kong University of Science and Technology. He is a co-author of the book *Digital Communications by Satellite* (New York: Wiley, 1981) and co-editor of the IEEE Press Book *Reed–Solomon Codes and Their Applications*. His research interests are in multi-media wireless communications.

Dr. Bhargava is very active in the IEEE and is the immediate Past President of the IEEE Information Theory Society. He was Co-chair for IEEE ISIT'95, Technical Program Chair for IEEE ICC'99 and is the General Chair of IEEE VTC'2002 Fall. He is a Fellow of the B.C. Advanced Systems Institute, Engineering Institute of Canada (EIC) and the IEEE. He is a recipient of the IEEE Centennial Medal (1984), IEEE Canada's McNaughton Gold Medal (1995), the IEEE Haraden Pratt Award (1999) and the IEEE Third Millennium Medal (2000).